

## Direct Imaging of Adsorption Sites and Local Electronic Bond Effects on a Metal Surface: C/Al(111).

H. BRUNE (\*), J. WINTTERLIN (\*), G. ERTL (\*) and R. J. BEHM (\*\*)

(\*) *Fritz-Haber-Institut der Max-Planck-Gesellschaft  
Faradayweg 4-6, D-1000 Berlin 33, West Germany*

(\*\*) *Institut für Kristallographie und Mineralogie, Universität München  
Theresienstr. 41, D-8000 München 2, West Germany*

(received 29 June 1990; accepted 23 July 1990)

PACS. 61.16 – Other determination of structures.

PACS. 68.20 – Solid surface structure.

PACS. 73.20 – Electronic surface states.

**Abstract.** – C atoms are adsorbed on an Al(111) surface in h.c.p.-type threefold hollow sites and significantly modify the charge density distribution in the surrounding Al atoms, as becomes evident from scanning tunnelling microscopy (STM) images resolving individual atoms of both the substrate and the adsorbate. Apparent modifications of the vertical positions of the Al atoms surrounding an adsorbate are not due to structural changes, but rather reflect local variations of their electronic structure induced by the chemical bond to the adsorbate, which lead to a decrease of the tunnel current at nearest neighbours and an increase at next-nearest neighbours, respectively.

Scanning tunnelling microscopy (STM) images reflect, to a first approximation, the distribution of charge density near  $E_F$  in front of the surface [1]. The presence of adsorbed atoms or small molecules generally causes changes of the electronic structure at and above the location of the adsorbate which, in turn, leads to modifications in the STM image [2]. The apparent size of an adsorbate in the STM image therefore does not necessarily correspond to the geometry of the adsorption complex, but predominantly results from electronic effects [2-5] and is therefore subject to variations in the experimental parameters tunnelling voltage and gap width [3]. Due to chemical bond effects such modifications are also expected at the surrounding substrate atoms, from where they are expected to rapidly decay with increasing distance from the adsorption site [3]. STM images with atomic resolution of substrate and adsorbate hence can identify the adsorption site as well as electronic modifications of the adjacent substrate atoms caused by the formation of the chemisorption bond. This will be demonstrated in the present letter for C atoms adsorbed on the close-packed Al(111) surface.

The experiments were performed with a «pocket size» microscope incorporated into an ultra high vacuum system ( $p_{\text{tot}} \leq 1 \cdot 10^{-8}$  Pa) with standard facilities for sample preparation and characterization [6]. The sample surface was cleaned by repeated cycles of annealing

(800 K, 2 min) and  $\text{Ar}^+$  ion bombardment ( $3 \mu\text{A}$ , 500 V, 30 min), until no contaminations were detected by Auger electron spectroscopy, and the LEED pattern showed sharp spots from the Al(111) substrate on a low background, indicative of a well-ordered surface. The tunnelling tip was electrochemically etched from polycrystalline W wire (0.7 mm diameter) and further cleaned in vacuum by field desorption. Prior to each STM experiment the tip was transferred into a high-resolution state by applying a short bias voltage pulse ( $(6 \div 9) \text{V}$ ) while scanning the surface. This method had been demonstrated to reproducibly provide atomic resolution STM images on Al(111) [6]. The images were recorded in the slow scan mode, at constant tunnel current and usually with the sample biased negatively, *i.e.* probing the occupied states near  $E_F$  of the sample. The grey scale used for representation of the STM images becomes darker with the tip closer to the surface plane.

STM images of the clean Al(111) surface resolve flat terraces with no additional structure at low tunnel currents ( $R_t \sim 10^9 \Omega$ ). Images recorded after exposing the surface to the residual gas background revealed new local features of identical shape which were randomly distributed over the surface, *i.e.* not condensed into islands or concentrated at steps. Their shape is evident from an STM image recorded under similar conditions (fig. 1), in which six of these features are resolved: central protrusions of  $0.3 \text{ \AA}$  height and  $4 \text{ \AA}$  diameter are surrounded by ringlike depression zones ( $0.2 \text{ \AA}$  depth,  $5.5 \text{ \AA}$  diameter). The density of these features in the STM images is strictly correlated with the intensity of a carbon signal in Auger spectroscopy, which identifies them as a carbon-containing species. Carbon originates from residual gas hydrocarbons which adsorb and decompose on the surface. The same structures were produced by mild sputtering (200 eV, 150 nA) in an ethylene atmosphere ( $\sim 10^{-6}$  mbar) and subsequent annealing. This procedure was found to be much more efficient than mere exposure to  $\text{C}_2\text{H}_4$  at  $T \geq 300 \text{ K}$ . On the basis of the thermal stability of these features—annealing to 700 K did not affect their typical shape in the STM images—they must result from atomically adsorbed carbon. Several carbon-containing molecules, adsorbed on Al(111), were shown to decompose below 700 K [7].

STM images recorded at narrower tip-surface separations in principle reproduced the shape of the  $\text{C}_{\text{ad}}$  atoms visible in fig. 1. Upon lowering the gap width, individual substrate atoms are resolved and the depression zone displays 6 minima as an additional structure. But only for extremely high-resolution conditions even the substrate atoms in the direct vicinity of the C adatom can be resolved, which are otherwise covered by the dominant protrusion. This is demonstrated in the two STM images in fig. 2, which except for a slight

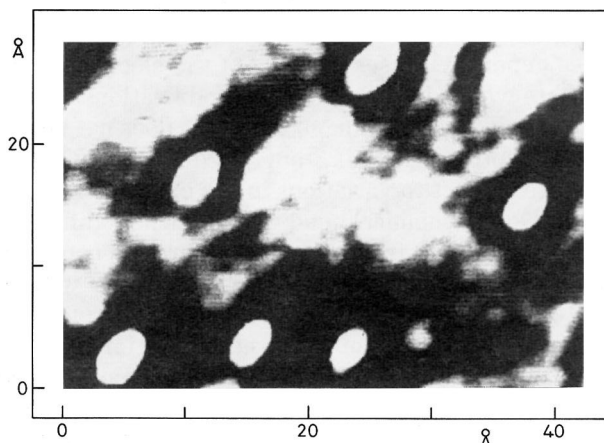


Fig. 1. – Detail of an STM image of a carbon-containing Al(111) surface ( $V_t = -500 \text{ mV}$ ,  $I_t = 1 \text{ nA}$ ). C adatoms are imaged as protrusions surrounded by a depression ring.

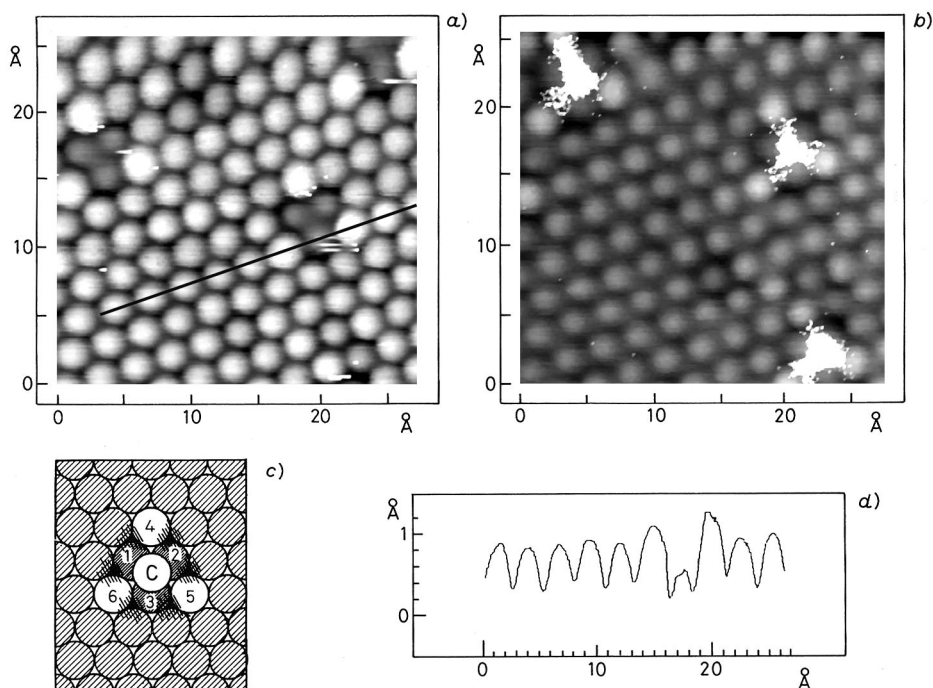


Fig. 2. – High-resolution STM images taken subsequently of (almost) the same Al(111) surface area, with two (three) carbon adatoms in the imaged area. *a)*  $V_t = -20$  mV,  $I_t = 41$  nA. *b)*  $V_t = -70$  mV,  $I_t = 41$  nA. *c)* Model of the atomic surrounding of a  $C_{ad}$ , 1-3: nn Al atoms, 4-6: nnn Al atoms. The marked hollow sites, surrounding atoms 1-3, are forming the dark depression ring in fig. 1. *d)* Cut along  $[1\bar{1}0]$  as indicated in *a)*.

lateral shift, due to thermal drift, both represent the same surface area. They only differ in the tunnelling conditions used during recording (fig. 2*a*):  $V_t = -20$  mV,  $I_t = 41$  nA, fig. 2*b*):  $V_t = -70$  mV,  $I_t = 41$  nA). This becomes evident from the identical relative geometry of the two characteristic sets of triangularly arranged, slightly protruding Al atoms in the central part of the images. Each of these sets in fact surrounds the location of an adsorbed carbon atom, which becomes obvious from fig. 2*b*). In this image protrusions at the centres of the respective sets indicate the positions of the C atoms. These protrusions are comparable to the ones described above, although the resolution is much better with the present image. The model in fig. 2*c*) gives a direct correlation between the shape of the  $C_{ad}$  features in lower-resolution images such as in fig. 1 and the atomic structure resolved in the images in fig. 2. The central protrusion in the former images is formed by the  $C_{ad}$ , and the depression ring originates from the threefold hollows marked as black dots in fig. 2*c*). With lower-resolution conditions similar features as the ones in fig. 1 were recorded also on the surface area imaged in fig. 2.

These images demonstrate that the Al atoms adjacent to the adsorbate are distinctly different from the more distant ones, which do not differ from those on the clean surface. The three nearest-neighbour (nn) Al atoms directly bound to the  $C_{ad}$  appear to be displaced downwards, while the three next-nearest-neighbour (nnn) Al atoms are apparently shifted upwards. As can be seen from the line scan reproduced in fig. 2*d*), these apparent displacements are of the order of about  $-0.3$  Å and  $+0.2$  Å, respectively. The data suggest that even the third-nearest neighbours are still slightly affected and exhibit again a weak depression.

The data in fig. 2 demonstrate that C atoms adsorb on the threefold hollows of the close-packed Al(111) surface. Furthermore, from the orientation of the triangular sets of prominent *nnn* Al atoms we can conclude that only one kind of threefold hollow sites is occupied: for h.c.p. or f.c.c.-type hollow sites, with an Al atom either one or two layers below, respectively, the orientation of these sets differs by  $60^\circ$ . Only one orientation was observed, which indicates the occupation of only one single type of adsorption site.

Even the nature of this site may be evaluated on the basis of the STM image reproduced in fig. 3. The nearly circular feature in the left half of the image represents a one-layer deep hole with an irregularly shaped border line. On the upper terrace four of the typical  $C_{ad}$ -induced triangular sets of Al atoms are visible. From the hexagonal lattice of white dots, which is constructed from the atomic positions of the second layer and extrapolated onto the first layer, it becomes evident that the adsorbed C atom is located at a site with another Al atom being present below. This means that the h.c.p.-type threefold hollow site has been identified as the location of adsorbed C atoms on Al(111). A threefold hollow site is very plausible in view of the general structural experience with atomic adsorbates [8-10], while the additional distinction between h.c.p. and f.c.c.-type site, on the other hand, is usually very difficult to achieve.

Cluster calculations for Al(100) revealed practically identical vertical positions for C and O atoms adsorbed on the fourfold hollow sites [11]. If we adopt these findings for Al(111), the C atom would be located in the threefold hollow site, about  $0.7 \text{ \AA}$  above the plane formed by the nuclei of the topmost Al atoms which is the position of adsorbed O atoms [9, 10]. However, the actual vertical height of the C atoms cannot be derived from the STM images. The shape of the C-induced features depends strongly on the tunnelling conditions. By changing the bias potential from  $-70$  to  $-20$  mV the central protrusion of about  $1 \text{ \AA}$  height, visible in fig. 2b), completely disappears, *i.e.* the adsorbed C atoms become virtually «transparent» to the STM (fig. 2a)).

For the Al atoms surrounding the adsorbate in the STM images it is very unlikely that the apparent vertical displacements are indeed due to geometric distortions, although such effects are in principle quite common with strongly bound adsorbates [8]. No substantial substrate lattice distortions, however, were found for ordered O overlayers on the densely packed Al(111) surface [9, 10], despite the very strong chemisorption bond. Recent calculations for isolated adatoms on Al(100) revealed, *e.g.*, that the Al atoms close to an adsorbed S atom are displaced laterally by about  $0.04 \text{ \AA}$  and vertically inwards by only about

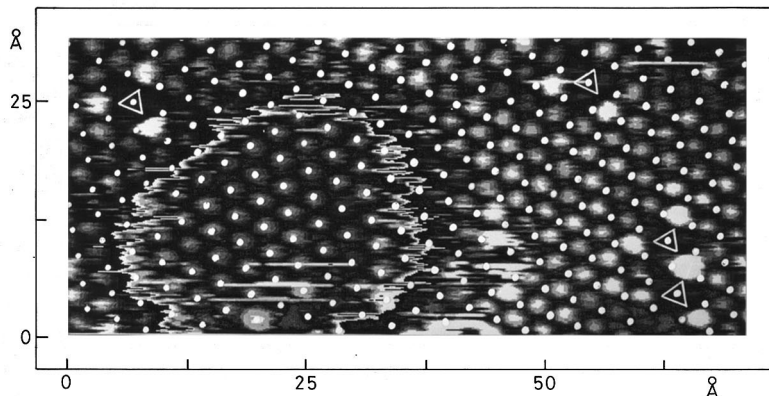


Fig. 3. – STM pattern of a surface area on Al(111), where a hole in the top layer allows to image atoms of the second layer too. Their lattice is extrapolated onto the first layer by white dots which mark h.c.p.-type adsorption sites there (f.c.c. sites remain dark). Four  $C_{ad}$  atoms are located at the h.c.p. sites marked by a triangle ( $V_t = -100$  mV,  $I_t = 100$  nA).



0.005 Å [12]. Such an effect would be outside the resolution limits of the STM and more than an order of magnitude smaller than the apparent displacements found here which are extending even to third-nearest neighbours. The quoted calculations exhibit, however, pronounced variations of the charge density contours. It is therefore concluded that the experimentally observed effects are primarily caused by the modification of the electronic structure of the substrate in the vicinity of the adsorbate: the electronegative C atom withdraws electronic charge from the neighbouring Al atoms (which therefore appear depressed in the STM image) in a similar way as reflected by the charge density contour plots calculated for O/Al(111) [10]. A Friedel-type oscillation of the charge density extending with decreasing amplitude from nearest neighbours (depletion) via next-nearest neighbours (accumulation) to third-nearest neighbours (depletion) is in full qualitative accord with model calculations performed by Lang and Williams [13] for electronegative adsorbates on a jellium surface.

This interpretation, in terms of charge density variations of the substrate atoms, is straightforward for STM images in the high-resistance regime like the one in fig. 1, where the Tersoff-Hamann formalism [1] is valid. In this case the STM trace closely resembles the local density of states (LDOS). For the images presented in fig. 2 and 3, however, it has to be pointed out that at the very narrow tip-surface separations in these images interactions between tip and sample come into play [4, 6, 14]. As a consequence the STM traces do not simply represent lines of constant charge density at  $E_F$  under these conditions. Nevertheless, also under these conditions the shape of the STM trace is determined by the electronic structure of the surface and local modifications therein, and the data reflect differences in the electronic structure for Al atoms on the bare surface and in the vicinity of adsorbed carbon. (Interestingly, the qualitative effect in the vertical displacements of these Al atoms clearly resembles that found for large gap with negligible tip-surface interactions.) Hence the results can be considered as direct experimental manifestation of the range over which neighbouring adsorbates may influence each other by indirect (*i.e.* mediated through the substrate) electronic interactions. These obviously reach to nn neighbours, in agreement with theoretical treatments which, in addition, also predict their oscillatory character [15].

Similar arguments apply for STM imaging of the C adatoms: their shape is similar to the features in fig. 1 over a wide range of tunnelling parameters, and effects like the transparency in fig. 2a) are confined to the very low distance regime. Accordingly, the former shape is assumed to be representative for the LDOS around  $E_F$ , while the drastic effects from changing the energy window around the contributing energy levels by just 50 meV in fig. 2 rule out a simple explanation in terms of LDOS around  $E_F$ . The spectral distribution of the surface density of states is not that sharply structured [5]. This effect is rather attributed to the variation in tip height—the data in fig. 2 were recorded with constant tunnelling current, *i.e.* varying distance. For the small tunnelling distances used for recording the images in fig. 2 interactions between tip and surface have to be considered and in addition interference effects between the wave functions of the tip and those of the C adatoms may occur [4]. Under these conditions small variations in the gap width can result in drastic changes in the STM trace. Most likely the observed transparency on the C atoms in fig. 2a) is due to these effects. Their contribution rapidly decay at larger distances. We recently found similar effects for adsorbed oxygen on Al(111), where similarly strong changes were observed if the tip height was varied, while upon variation of the bias voltage (at fixed distance) this effect was much smaller.

In summary we have presented STM images of individual carbon adatoms on an Al(111) surface, where the atomic resolution of both substrate and adsorbate atoms (on different terraces) allows direct conclusions on the adsorption site (h.c.p.-type threefold hollow) and on the lateral range of the electronic modification of the surrounding Al surface atoms

induced by the presence of the carbon adatom. They directly reflect the local electronic deformation of a metal surface associated with the chemical bond to the adatom.

\* \* \*

We gratefully acknowledge discussions with P. FEIBELMAN and G. DOYEN.

#### REFERENCES

- [1] TERSOFF J. and HAMANN D., *Phys. Rev. B*, **31** (1985) 805.
- [2] LANG N. D., *Phys. Rev. Lett.*, **55** (1985) 230.
- [3] STROSCIO J. A., FEENSTRA R. M. and FEIN A. P., *Phys. Rev. Lett.*, **58** (1987) 1668.
- [4] KOPATZKI E., DOYEN G., DRAKOVA D. and BEHM R. J., *J. Microsc.*, **152** (1988) 687.
- [5] LANG N. D., *Phys. Rev. Lett.*, **58** (1987) 45.
- [6] WINTERLIN J., WIECHERS J., BRUNE H., GRITSCH T., HÖFER H. and BEHM R. J., *Phys. Rev. Lett.*, **62** (1988) 59.
- [7] CHEN J. G., BASU P., NG L. and YATES J. T., *Surf. Sci.*, **194** (1988) 397.
- [8] MCLAREN J. M., PENDRY J. B., ROUS P. J., SALDIN D. K., SOMORJAI G. A., VAN HOVE M. A. and VVEDENSKY D. D., *Surface Crystallographic Information Service: A Handbook of Surface Structures* (D. Reidel, Dordrecht) 1987.
- [9] See e.g. BATRA I. P. and KLEINMAN L., *J. Electron Spectrosc. Rel. Phenom.*, **33** (1984) 175.
- [10] WANG D., FREEMAN A. J. and KRAKAUER H., *Phys. Rev. B*, **24** (1981) 3092.
- [11] MÜLLER J. E., *Surf. Sci.*, **178** (1986) 589.
- [12] FEIBELMAN P., *Phys. Rev. Lett.*, **63** (1989) 2488.
- [13] LANG N. D. and WILLIAMS A. R., *Phys. Rev. B*, **18** (1978) 616.
- [14] CIRACI S., BARATOFF A. and BATRA I. P., *Phys. Rev. B*, **41** (1990) 2763.
- [15] EINSTEIN T. L. and SCHRIEFFER J. R., *Phys. Rev. B*, **7** (1973) 3629; LAU K. H. and KOHN W., *Surf. Sci.*, **75** (1978) 69.